Delamination of plasters applied to historical masonry walls: analysis by acoustic emission technique and numerical model

Delamination of plasters applied to historical masonry walls: analysis by acoustic emission technique and numerical model

A Grazzini[1,2], G Lacidogna[1], S Valente[1] and F Accornero[1]

[1]Department of Structural, Geotechnical and Building Engineering, Politecnico di Torino, Corso Duca degli Abruzzi 24, Turin, Italy

E-mail: alessandro.grazzini@polito.it

Abstract. Masonry walls of historical buildings are subject to rising damp effects due to capillary or rain infiltrations, which in the time produce decay and delamination of historical plasters. In the restoration of masonry buildings, the plaster detachment frequently occurs because of mechanical incompatibility in repair mortar. An innovative laboratory procedure is described for test mechanical adhesion of new repair mortars. Compression static tests were carried out on composite specimens stone block-repair mortar, which specific geometry can test the de-bonding process of mortar in adherence with a stone masonry structure. The acoustic emission (AE) technique was employed for estimating the amount of energy released from fracture propagation in adherence surface between mortar and stone. A numerical simulation was elaborated based on the cohesive crack model. The evolution of detachment process of mortar in a coupled stone brick–mortar system was analysed by triangulation of AE signals, which can improve the numerical model and predict the type of failure in the adhesion surface of repair plaster. Through the cohesive crack model, it was possible to interpret theoretically the de-bonding phenomena occurring at the interface between stone block and mortar. Therefore, the mechanical behaviour of the interface is characterized.

1. Introduction

The historical masonry walls have original plasters often in phase of separation because of climatic conditions as rain infiltrations and damp capillary action. The restoration work needs the application of new dehumidified mortars. The great variety of historical masonry textures requires preliminary tests to assess the structural compatibility of the dehumidified mortars suitable for brick surfaces [1].

The authors have developed a new experimental methodology to assess the mechanical adhesion of new dehumidified mortars applied to historical masonry surfaces. This experimental methodology was carried out at the Politecnico Laboratory, and tested at the Sacro Monte di Varallo, one of the most famous UNESCO heritage site in Italy [2]. This historical site, whose construction has been extended from the 15th to the 18th century, contains 45 chapels that show the Christ's life by particular frescoes and sculptures (figure 1). The main problem of historical plasters' preservation is linked to the rain infiltrations and to the freezing-thawing cycles that compromise their adhesion to stone masonries. Through compression static tests on stone-mortar composite specimens, it was possible to prequalify the dehumidified mortar with greater durability guarantees. Sometime the long-term detachment determined the failure of the restoration work. The test validates the mechanical compatibility between the repair mortars and historical masonries stone, as a guarantee also for durability over time against atmospheric agents. The Acoustic Emission (AE) monitoring technique was employed during static

tests for assessing damage evolution inside the adherence surface [3,4].

Figure 1. Chapel of the Christ at the court of Herod.

2. Materials and experimental setup

For carrying out tests, a particular geometry of the composite specimen has been proposed. Four mixed specimens were made, applying a 40 mm mortar layer to both shorter faces of the stone brick suitably cut with the dimensions shown in figure 2(a). The mechanical characteristics of the repair mortar and the stone brick were chosen equivalent to those of the stone masonry at the Sacro Monte di Varallo. The hydraulic lime mortar was a pre-blended transpiring product, for dehumidifying repair work on historical masonry damaged by dampness. For this mortar the Young's modulus was 7000 MPa, the compressive strength was 33.8 MPa.

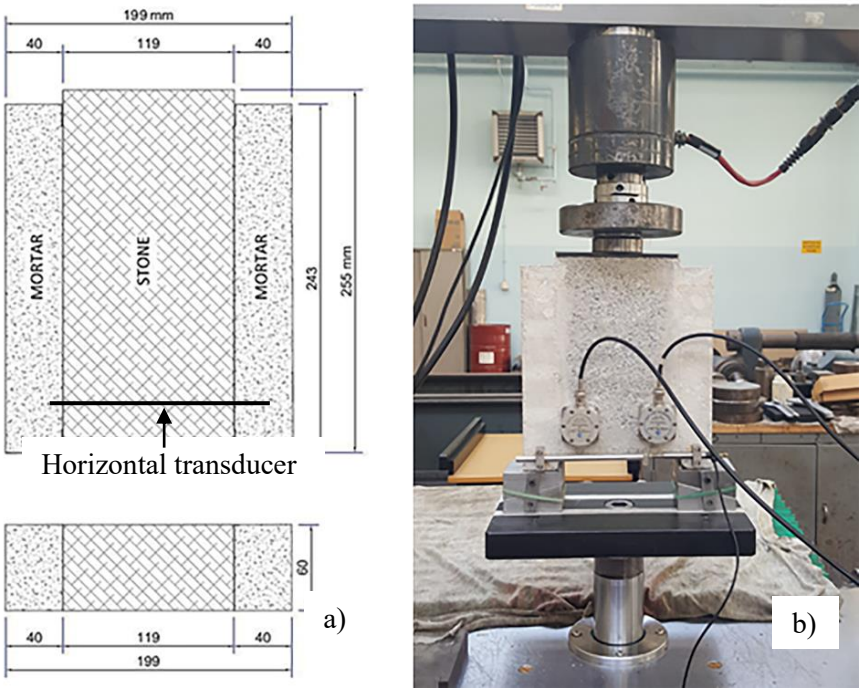

Figure 2. Geometry of composite specimen (a) and test setup (b).

The surface of the stone block has been treated specifically by means of a drill to facilitate the mortar's adhesion. This treatment aimed to simulate the real discontinuities on the wall surface that favor the adhesion of the plaster. The application of the dehumidified mortar took place leaving specific and surface symmetrical discontinuities at the top and bottom of the specimen, as showed in figure 2(a). These notches favored the trigger and propagation of multiple cracks, in order to test the adhesion of two linked materials. An inductive horizontal displacement transducer was applied at the bottom of the specimen for the bulging displacements (figure 2(b)). The vertical displacements were recorded by the piston's translation of the 250 kN servo controlled test machine. The composite specimens were tested by monotonous compression load by horizontal controlled opening. Static tests have been performed after 28 days of maturation. The composite specimen rested, through the side layers mortar, on a double system of steel wedges (figure 3). The wedges were coupled by a 1 mm thick Teflon layer for reducing the horizontal friction during the plaster's expansion. The "SM" (Stone brick-Mortar) label has been associated with each specimen with its sequence number.

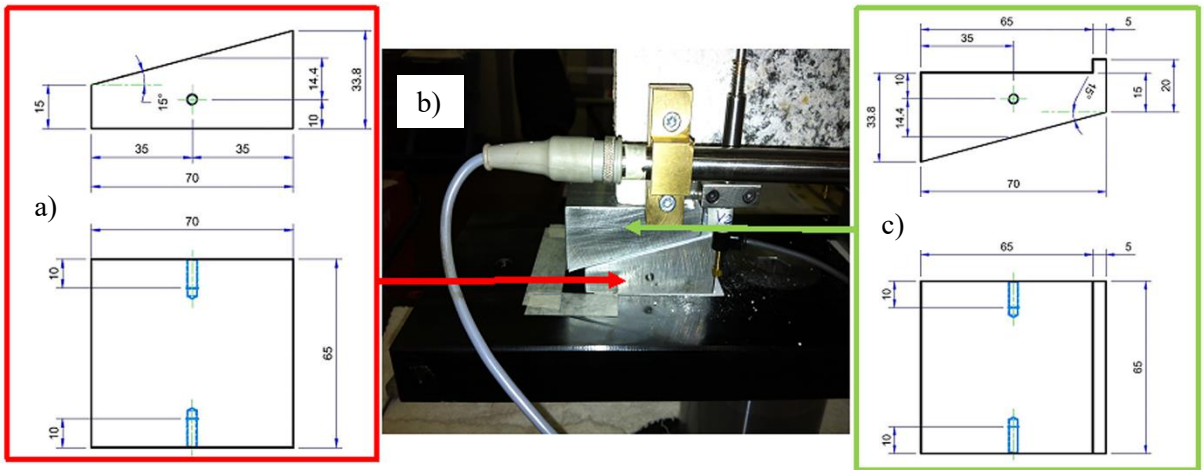

Figure 3. The wedges' geometry (a – c) and test setup (b).

3. Acoustic emission monitoring

As regards the AE monitoring, the microcracks propagation generated AE signals that were detected by dedicated sensors applied to the external specimens surface. The AE waves were amplified with a gain of 60 dB before they have been analyzed, fixing the threshold level detection up to 2 mV. The AE sensors were attached to the specimens by means of a silicon glue. In this way it was possible to guarantee a good contact between the sensor and the specimen, also during the final crack phases.

The AE measurement system was able to recorder each signal waveforms. Rise time and peak amplitude were the AE parameters used to classify active cracks. The shape of the AE waveforms distinguishes the fracture mode: typical shear events are usually characterized by long rise times and high amplitudes, instead low rise time are distinctive of tensile crack propagations. In particular the rise angle (RA), that shows these conditions, was calculated as the ratio of the rise time to the peak amplitude. The first is expressed in ms, the second one in V [3].

Moreover, in order to distinguish the cracking mode, the Average Frequency (AF) expressed in kHz was also used. The AE ringdown count is the number of crossings threshold along the duration time. The ratio between the AE ringdown count and the duration time of each signal gives the AF values. The change of the cracking mode from tensile to shear is followed by the shift from higher to lower values of AF [3]. Nevertheless, when large cracks (Mode I) are forming, the frequency attenuation could be a function of this discontinuity. The wavelength of the AE signals should be larger of these discontinuities to make the waves pass through, therefore the frequencies' shift from higher to lower values could show also a dominant tensile cracking mode.

For the sake of synthesis, the results of the AE monitoring were presented only for specimen SM4.

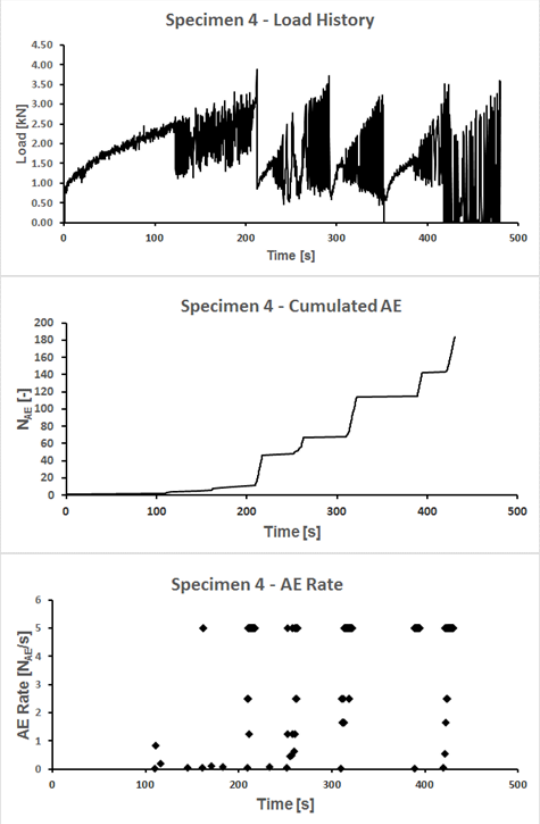

Figure 4. Specimen SM4: Load vs time diagram, Cumulated AE, and AE rate.

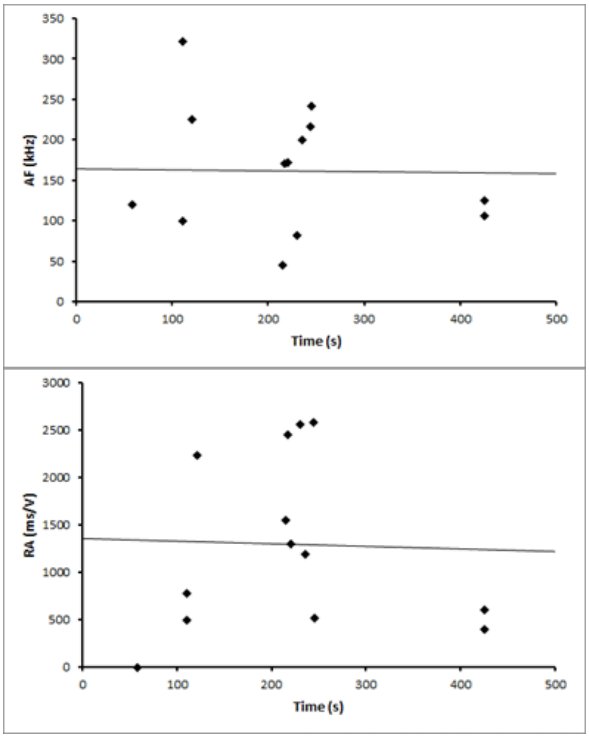

Figure 5. Specimen SM4: Average Frequency (AF) vs time, and Rise Angle (RA) vs time.

The load vs. time diagram of the specimen SM4 is shown in figure 4, together with AE cumulated curve, and AE rate. During the first part of the test, when the load increases proportionally over time, there are few AE signals. However, a clear growth in the AE hits is obtained in the correspondence of each sharply decrease of the load vs. time curve. This supports the fact that the AE signals are mainly associated with the energy emitted by the specimen during the delamination of the mortar from the stone block (snap-back instabilities) [5].

Using the ordinary least squares method, the linear regression of the signal frequencies (AF) and the signals rise angles (RA) were traced during the whole test. Considerable variations from the mean trend were observed in particular immediately after 100 seconds from the beginning of the test, around 200 seconds, and around 420 seconds towards the end of the test (figure 5). In the first phase, from 0 to 120 seconds, rise angles with low values prevail, while the frequencies are oscillating with the higher values more distant from the average trend. This indicates a prevalent Mode I in the delamination process in the initial loading phase. In the second phase, the highest values of the RAs during the whole test were obtained, while the frequencies continue to oscillate with the lowest values more distant from the average. This behavior shows how the delamination process that leads to collapse develops with sudden stress drops and is mainly accompanied by the sliding of the mortar with respect to the stone block (Mode II). In the final phase, over 400 seconds, the frequencies are still lowered below the average line, while the RAs once again become low, so it can be said that there is no prevailing fracture mode before the specimen collapses definitively.

4. Numerical simulation

The Barenblatt – Dugdale - Hillerborg model, also known as the cohesive crack model, is a good numerical approach to simulate the behaviour of quasi-brittle materials, as the stone-mortar

delamination. The crack initiation criterion is assumed as:

$$\left(\frac{\sigma_0}{f_t}\right)^2 + \left(\frac{\tau_0}{f_s}\right)^2 = 1 \quad (1)$$

where σ_0 and τ_0 are the stresses respectively orthogonal and tangential directions, f_t and f_s are the respective strengths. The fictional crack tip is the point where equation (1) is proved. The cohesive stresses present on the non-linear fracture process zone (FPZ) are decreasing functions of the effective value of the displacement discontinuity w_{eff} [6-11]. It was assumed:

$$w_{\text{eff}} = \sqrt{\left(\frac{w_n}{w_{\text{nc}}}\right)^2 + \left(\frac{w_t}{w_{\text{tc}}}\right)^2} \quad (2)$$

where w_n is the first component of the mutual-orthogonal displacement, and w_t is the second one (tangential to the interface); the related critical values are w_{nc} and w_{tc}. If $w_{eff} > 1$ there is no stress transfer and the crack is stress free; otherwise, the stresses are decreasing functions of w_{eff} that follow a pre-defined softening law. The above mentioned law is assumed [12]:

$$\frac{\sigma}{\sigma_0} = \frac{\tau}{\tau_0} = \left[1 - \frac{1-\exp(-\alpha \cdot w_{\text{eff}})}{1-\exp(-\alpha)}\right] \quad (3)$$

where $\alpha = 5$ is assumed. Real crack tip is called the point where $w_{eff} = 1$. Outside the FPZ the material had a linear-elastic behavior. The fracture process starts symmetrically, but loses this property afterwards [13-15] because of the propagation of the round-off errors. In this case the numerical simulation was controlled according a uniform downward velocity to the upper edge on the rock. This choice was able to prevent the growth of the round-off errors so that, from an engineering point of view, the propagation of the two cohesive cracks occurs symmetrically. The interface strength properties were assumed as shown in tables 1 and 2. The numerical analyses were performed using the ABAQUS [16] code. Figure 6 shows the deformed mesh of finite element model.

Table 1. The interface strength properties.

f_t (N/mm^2)	f_s (N/mm^2)	w_{nc} (mm)	w_{tc} (mm)
0.8	1.0	0,015	0,015

Table 2. Mechanical characteristics of materials.

	Young's modulus (N/mm^2)	Poisson ratio
Mortar	7000	0.15
Rock	35000	0.20

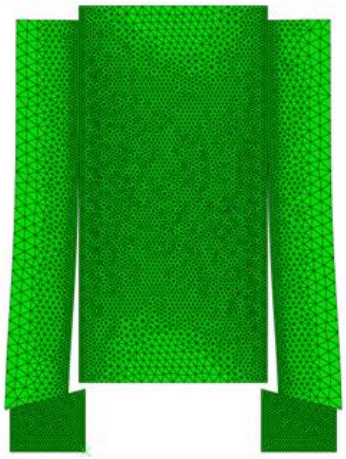

Figure 6. Finite element deformation during max displacement.

5. Numerical and experimental outcomes

The adherence between the repair plaster and masonry stone was tested by the notch tips. The experimental procedure simulated the fatigue loads that can compromise the service-life of a dehumidified plaster. The experimental results shows four stress singularity points in the stone-mortar specimens: two notch tips at the top, and two at the bottom (see figure 2). These are the weakest points involved in the singular stress fields. During the tests, it was possible to observe that the cracks beginning from the bottom were faster than the cracks from the top, because of the wedges. The friction, reduced by the teflon sheet, is not taken into account in the numerical simulation and the materials are considered homogeneous. This is the reason why the response curve is continuous (see figure 7). On the contrary, the properties of the rock specimen can change from point to point. This is the reason why the experimental curve shows many discontinuities (see figure 7). The numerical model represents an ideal behaviour which, in particular in the early stages of loading, fit the average values of the experimental curves, but it is not able to identify the snap-back instabilities that experimentally occur during the delamination process.

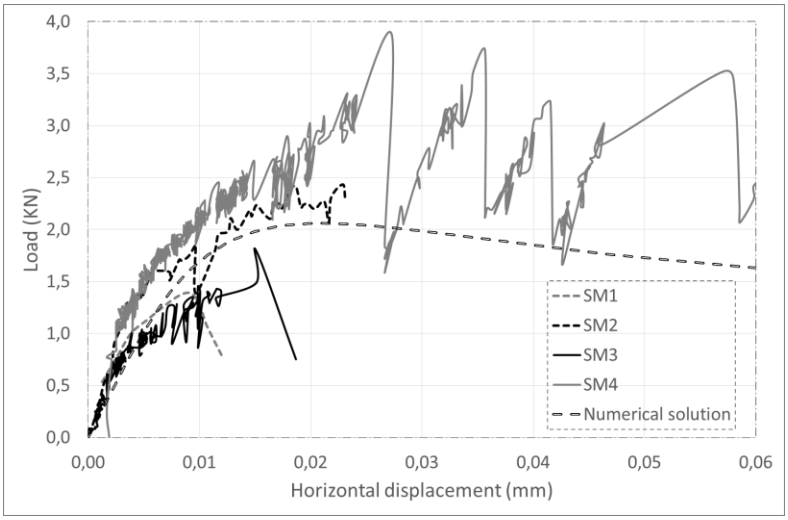

Figure 7. Load – horizontal displacement curves of the specimens vs. the numerical solution.

6. Conclusions

- The aim of this test was to pre-qualify the most durable dehumidified mortar which mechanical compatibility to the historical masonry can avoid delamination problems by dampness and hygrometric effects.
- The experimental procedure, performed by mixed specimens, allowed testing the adherence between the dehumidified repair plaster and the historical masonry stone. This procedure was able to produce in static tests the same interface stresses that caused by freeze and thaw actions.
- The AE signals were associated with the energy emitted by the specimens in the delamination phase between the mortar and the stone block. The variation of the AE parameters (AF and RA) depends strictly on the type of specimen damage.
- From the obtained results it was possible to identify a prevalent Mode I in the delamination process during the initial loading phases. As the test goes on, the delamination process develops with sudden load drops, mainly accompanied by the sliding of the mortar with respect to the stone block (Mode II). While, in the final loading phase, no prevalent fracture mode has emerged before the specimen definitively collapses.
- The non-linear phenomena that occur at the interface between mortar and stone during the de-bonding process were theoretically interpret by means of the cohesive crack model.

References

[1] Bocca P and Grazzini A 2013 *J Mat Civ Eng* **25** 274-80
[2] Bocca P, Valente S, Grazzini A and Alberto A 2014 *Int J Arch Her* **8** 336-48
[3] Carpinteri A, Lacidogna G, Accornero F, Mpalaskas F, Matikas A and Aggelis D 2013 *Cemente Concr Comp* **44** 9-16
[4] Carpinteri A, Grazzini A, Lacidogna G and Manuello A 2014 *Str Contr Health Monit* **21** 950-61
[5] Carpinteri A and Accornero F 2017 *Eng Fract Mech* doi: 10.1016/j.engfracmech.2017.11.034
[6] Cervenka J, Kishen J M C and Saouma V E 1998 *Eng Fract Mech* **60** 95-107
[7] Barpi F and Valente S 2010 *Eng Fract Mech* **77** 2182-91
[8] Barpi F and Valente S 2002 *Int J Num Anal Meth Geomech* **26** 1005-27
[9] Barpi F and Valente S 2004 *Int J Sol Str* **41** 2607-21
[10] Barpi F and Valente S 2005 *Eng FractMech* **72** 2427-43
[11] Barpi F and Valente S 2008 *Eng Fract Mech* **75** 629-42
[12] Cornelissen H A W, Hordijk D A and Reinhardt H W 1986 *Heron* **31** 45-56
[13] Barpi F and Valente S 1998 *Int J Sol Str* **35** 1851-61
[14] Alberto A, Antonaci P and Valente S *Proc. 11th Int. Conf. Mech Beh Mat* 1151-6
[15] Bocca P, Grazzini A, Masera D, Alberto A and Valente S 2011 *J Phys Conf Series* **305**
[16] Dassault System Simulia Corp., Providence, RI, ABAQUS, release 6.10, 2010